Influence of long-range cation order on relaxor properties of doped $Pb(Mg_{1/3}Nb_{2/3})O_3$ ceramics

X. Zhao, W. Qu, and X. Tan*
Department of Materials Science and Engineering, Iowa State University, Ames, Iowa 50011, USA

A. A. Bokov and Z.-G. Ye*
Department of Chemistry, Simon Fraser University, Burnaby, British Columbia, Canada V5A 1S6
(Received 17 December 2008; revised manuscript received 27 February 2009; published 2 April 2009)

The 1:1 *B*-site cation order in $Pb(Mg_{1/3}Nb_{2/3})O_3$ relaxor ferroelectric ceramics was significantly enhanced by doping of minor amounts of La^{3+}, Sc^{3+}, or W^{6+} (less than 3 at. %) combined with a slow cooling procedure. Transmission electron microscopy examination confirmed the size increase of the cation-ordered regions embedded in a disordered matrix in the samples that were slowly cooled after sintering. The average cation ordering parameter (S) determined from x-ray diffraction data in these partially ordered samples was about 0.3–0.4. The ferroelectric properties and dielectric relaxation were compared in partially ordered and disordered ($S=0$) samples with the same composition. It was found that typical relaxor behavior was preserved in partially ordered ceramics. Furthermore, the temperature and diffuseness of the characteristic relaxor permittivity peak and the parameters of dielectric relaxation (in particular, the distribution of relaxation times and the Vogel-Fulcher freezing temperature) were practically independent of S. In contrast, the diffuseness of the phase transition from the ferroelectric phase (induced by external electric field) to the ergodic relaxor phase appeared to be much larger in the disordered samples than in the partially ordered ones (this diffuseness was assessed using pyroelectric current and ferroelectric hysteresis loops). These results suggest that cation ordering did not influence the behavior of polar nanoregions which are responsible for the dielectric response in the ergodic relaxor phase but significantly influenced the ferroelectric phase transition. The results are interpreted in terms of different types of polar regions in the disordered matrix and cation-ordered domains.

DOI: 10.1103/PhysRevB.79.144101 PACS number(s): 77.22.Gm, 77.80.−e, 64.60.fh, 77.84.Dy

I. INTRODUCTION

Complex perovskite $Pb(Mg_{1/3}Nb_{2/3})O_3$ (PMN) has been extensively investigated since 1958 due to its unique relaxor ferroelectric behavior.[1–4] Ferroelectric domains in PMN manifest themselves as polar nanoregions (PNRs), which nucleate at the Burns temperature $T_B \approx 650$ K. Upon cooling the PNRs begin to grow, reaching about 7 nm at 10 K, with the most significant growth taking place around the intrinsic Curie temperature $T_{C0}=213$ K. The structure of the polar regions is slightly distorted along the ⟨111⟩ direction, yet the long-range structure preserves cubic symmetry without any phase transition down to liquid helium temperature. The polar axis of these nanodomains is randomly fluctuating among several directions.[3] The PNRs can grow into micrometer sized ferroelectric domains under external electric fields during cooling, which corresponds to a first-order relaxor to normal ferroelectric phase transition.[5–12] Relaxation of PNRs accounts for the characteristic dielectric behavior of relaxors in which unusually large and diffuse maximum is observed on the temperature dependence of dielectric permittivity, while the relaxation rate follows the Vogel-Fulcher (VF) temperature dependence (in contrast to Arrhenius dependence in normal dielectrics).

It is believed that the relaxor behavior of PMN is associated with the 1:1 *B*-site cation order.[13,14] The cation-ordered domains, ranging from 2 to 5 nm in size, are embedded in the disordered matrix and do not grow upon thermal treatment. In the ordered domains every other {111} plane of the *B*-site sublattice is solely occupied by Nb cations (referred to as the β'' sublattice), while the other {111} plane is randomly occupied by Mg and the rest of Nb cations (referred to as the β' sublattice). This "random site model"[15] keeps the composition the same and preserves the charge neutrality in the ordered and disordered regions. It is suggested that the growth of the cation-ordered domains in PMN is constrained by kinetic limitations.

Generally cation ordering is expected to influence relaxor properties. Indeed, relaxor ferroelectrics are found among disordered crystals. In the $Pb(B'_{1/2}B''_{1/2})O_3$-type complex perovskite crystals, variation in the order degree of B' and B'' cations (by means of high-temperature treatment) can lead to dramatic changes in ferroelectric behaviors. Namely, the relaxor behavior is characteristic of disordered samples, while a normal (sharp) ferroelectric or antiferroelectric phase transition is observed in samples of the same composition with long-range cation order.[3,16–22] In contrast, the $Pb(B'_{1/3}B''_{2/3})O_3$-type perovskite relaxors show diffuse permittivity peaks with pronounced relaxor dielectric dispersion even in samples with large cation-ordered domains.[15] Relaxor behavior is related, in this case, to the fact that the β' sublattice still remains chemically disordered as suggested by the random site model. However, mechanisms underlying the relation between the structures of cation-ordered domains, polar domains, and ferroelectric properties are not understood thoroughly so far in these $Pb(B'_{1/3}B''_{2/3})O_3$-type oxides.

The limitations on the growth of cation-ordered domains in PMN can be largely overcome by chemical modification. For example, La^{3+} (>4 at. %) or Sc^{3+} doping (>5 at. %) has been reported to enhance the degree of cation order in PMN.[23–27] W^{6+}, when incorporated in PMN at >10 at. %, can also lead to the development of long-range cation order.[28] In the present work we demonstrate that, combined

with appropriate thermal treatment, only 2 or 3 at. % doping of La^{3+}, Sc^{3+}, or W^{6+} can develop large cation-ordered domains in PMN ceramics. To determine the relation between the cation order and relaxor ferroelectric properties, we compare ordered and disordered samples of the same composition in terms of structure and properties. The main conclusions are expected to be general for other relaxor ferroelectric compounds of the $Pb(B'_{1/3}B''_{2/3})O_3$ type.

II. EXPERIMENTAL PROCEDURE

La^{3+}, Sc^{3+}, and W^{6+} were introduced into PMN separately at a level of 2 or 3 at. % through forming solid solutions of $Pb(Mg_{1/3}Nb_{2/3})O_3$ with

$$La(Mg_{2/3}Nb_{1/3})O_3,$$

$$Pb(Sc_{1/2}Nb_{1/2})O_3,$$

and

$$Pb(Mg_{1/2}W_{1/2})O_3.$$

The detailed chemical formulae are as follows:

$$0.97Pb(Mg_{1/3}Nb_{2/3})O_3 - 0.03La(Mg_{2/3}Nb_{1/3})O_3(\text{referred to as La3}),$$

$$0.94Pb(Mg_{1/3}Nb_{2/3})O_3 - 0.06Pb(Sc_{1/2}Nb_{1/2})O_3(\text{referred to as Sc3}),$$

$$0.96Pb(Mg_{1/3}Nb_{2/3})O_3 - 0.04Pb(Mg_{1/2}W_{1/2})O_3(\text{referred to as W2}).$$

Ceramic samples were prepared with the columbite method developed by Swartz and Shrout.[29] High-purity (>99.9 wt. %) oxide powders of PbO, MgO, Nb_2O_5, La_2O_3, Sc_2O_3, and WO_3 were used as starting materials. Before weighing and mixing, the powders were baked at high temperatures to remove moisture and organic impurities to ensure precise stoichiometry. The *B*-site oxide powders were first mixed and milled with yttrium stabilized zirconia media (Tosoh, OH, USA) in isopropyl alcohol within plastic bottles on a vibratory mill for 3 h. Next, the mixed stoichiometric powders were calcined at 1100 °C for 4 h in alumina crucibles. The calcined powders were then mixed with PbO and/or La_2O_3 powders, milled for 3 h, and calcined at 900 °C for 4 h to form phase pure perovskite powders. A uniaxial pressure of 150 MPa was applied to the perovskite powder, which contained polyvinyl alcohol binder (2 wt. % aqueous solution), to form pellets. The pressed pellets were then buried in PMN protective powder and sintered at various temperatures (1200–1250 °C) for 3 h. A heating/cooling ramp rate of 600 °C/hour was used to obtain "disordered" samples. To obtain "ordered" samples, a much slower cooling rate (10 °C/hour) was applied from the sintering temperature down to 900 °C. These slow-cooled samples are referred to as "La3 ordered," "Sc3 ordered," and "W2 ordered," respectively. A pellet of pure PMN was also prepared with the slow-cooling procedure as a reference sample.

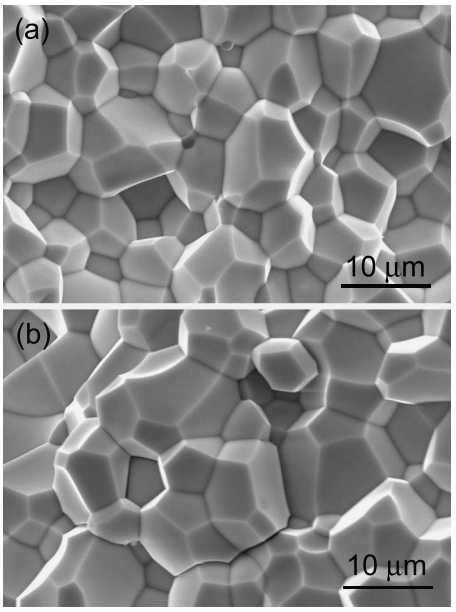

FIG. 1. SEM micrographs of the fracture surfaces of the (a) La3-ordered and (b) Sc3-ordered samples.

After the surface layer was removed, the density of these ceramics was measured by the Archimedes method and the grain size was examined by scanning electron microscopy (SEM). X-ray diffraction tests were performed on sintered pellets to check the phase purity and the degree of cation order. The cation-ordered domains were also directly imaged with the dark field technique using a transmission electron microscope (CM30, Philips, The Netherlands). Dielectric characterization was carried out with an *LCR* meter (HP-4284A, Hewlett-Packard) in conjunction with an environmental chamber (9023, Delta Design). A heating/cooling rate of 2 °C/min was used during the measurements. The thermal depolarization current was measured during zero-field heating with a picoammeter (Model 486, Keithley) from the field-cooled (10 kV/cm) samples. The polarization hysteresis was measured with a standardized ferroelectric test system (RT-66A, Radiant technologies). The relative dielectric permittivity in a wider frequency range of 10^{-2}–10^5 Hz was measured with an impedance analyzer (Novocontrol system, Novocontrol technologies), which includes an Alpha high-resolution dielectric analyzer and the Quatro cryosystem for temperature control.

III. RESULTS

A. Cation order in ceramics

Density measurements show that all ceramic samples have a relative density in the range of 92–96%. SEM examination confirmed the high relative density and revealed the grain size of the ceramics. Figure 1 shows the SEM micrographs of the La3-ordered and Sc3-ordered ceramics, from which the average grain size is determined. The grain size of all ceramics is listed in Table I, where all the doped ceramics were found to have similar values.

TABLE I. The structure of pure and La^{3+}, Sc^{3+}, and W^{6+}-doped PMN ceramics.

Composition	Relative density (%)	Lattice parameter (Å)	Grain size (μm)	Cation ordering parameter
PMN	94	4.0481	14.5	0
La3	94	4.0468	5.5	0
La3 ordered	93	4.0458	5.5	0.4
Sc3	96	4.0486	4.0	0
Sc3 ordered	92	4.0483	7.0	0.4
W2	94	4.0462	5.0	0
W2 ordered	93	4.0471	5.0	0.3

X-ray diffraction experiments indicate a pure perovskite phase in all ceramics. In the La3-ordered, Sc3-ordered, and W2-ordered samples (which were slowly cooled after sintering), the (1/2 1/2 1/2) superlattice peak appears, as shown in Fig. 2. This peak is practically absent in pure PMN ceramics and in rapidly cooled La3, Sc3, and W2 samples. The presence of the (1/2 1/2 1/2) superlattice peak in complex perovskites is an indication of the development of 1:1 *B*-site cation order.[24] Therefore, the cation order in PMN can be enhanced significantly even with only 2 or 3 at. % level chemical modification. Following the common procedure used in literature,[15,24] the cation ordering parameter S is evaluated from the (1/2 1/2 1/2) superlattice peak intensity based on the random site model and is listed in Table I. In the evaluation, Mg^{2+} and Sc^{3+} are assumed to occupy only the β' sublattice, while W^{6+} is assumed to occupy only the β'' sublattice, i.e., $Pb_{0.97}La_{0.03}[(Mg_{2.06/3}Nb_{0.94/3})_{1/2}(Nb)_{1/2}]O_3$, $Pb[(Mg_{1.88/3}Sc_{0.06}Nb_{0.94/3})_{1/2}(Nb)_{1/2}]O_3$, and $Pb[(Mg_{0.68}Nb_{0.32})_{1/2}(Nb_{0.96}W_{0.04})_{1/2}]O_3$ are assumed for La3, Sc3, and W2, respectively. The ratio of the peak intensity of the experiment to the calculated peak intensity based on these assumed complete ordering models equals to the square of the ordering parameter S.

The enhanced cation order in the slowly cooled ceramic samples is further confirmed by transmission electron microscopy (TEM) analysis. Figure 3 shows dark field images formed with the (1/2 1/2 1/2) superlattice spot in the ⟨110⟩-zone axis selected area electron diffraction pattern. Large cation-ordered domains were observed in all the slowly cooled ceramics. The size of these cation-ordered domains is about 100 nm for both La3 ordered and Sc3 ordered ceramics, while slightly smaller (~40 nm) for the W2-ordered ceramic. The TEM results are consistent with the calculated ordering parameter listed in Table I.

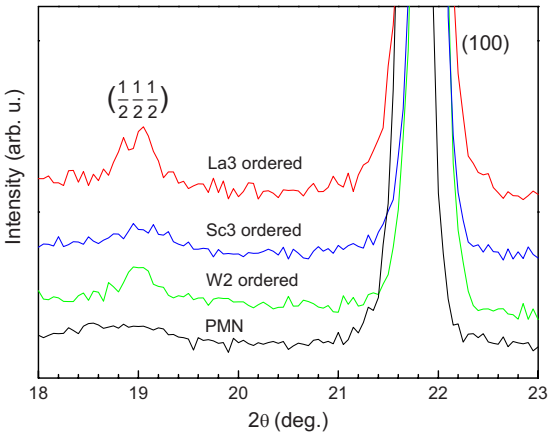

FIG. 2. (Color online) Partial x-ray diffraction spectra of La3-ordered, Sc3-ordered, and W2-ordered samples revealing the (1/2 1/2 1/2) superlattice peak at ~19°. Data for PMN ceramics are included for reference.

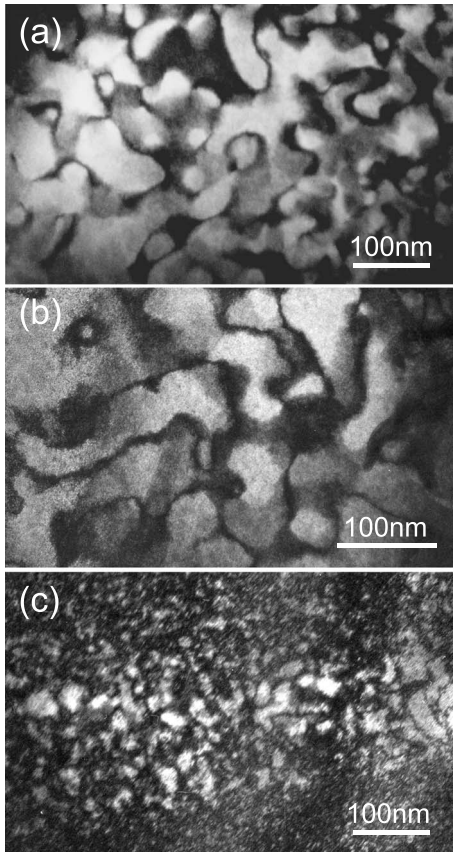

FIG. 3. TEM dark field micrographs of 1:1 cation-ordered domains formed with the (1/2 1/2 1/2) superlattice spot in the ⟨110⟩-zone axis selected area electron diffraction pattern. (a) La3 ordered, (b) Sc3 ordered, and (c) W2 ordered.

B. Dielectric properties

The relative dielectric permittivity (ε') of these ceramics as a function of temperature was measured at 100 Hz, 1 kHz, 10 kHz, and 100 kHz. As shown in Fig. 4, all disordered and ordered samples exhibit a broad relative dielectric permittivity peak with strong frequency dispersion, indicating that the relaxor ferroelectric behavior is preserved even in the samples with large domains of cation order. The four plots in Fig. 4 were presented with the same scale for direct visual comparison. It is evident that doping with La^{3+} (significantly) and with W^{6+} (slightly) suppresses the dielectric permittivity. In contrast, doping with Sc^{3+} enhances the permittivity. At the same time, the development of long-range cation order in W^{6+}-doped PMN can slightly recover the suppressed dielectric permittivity.

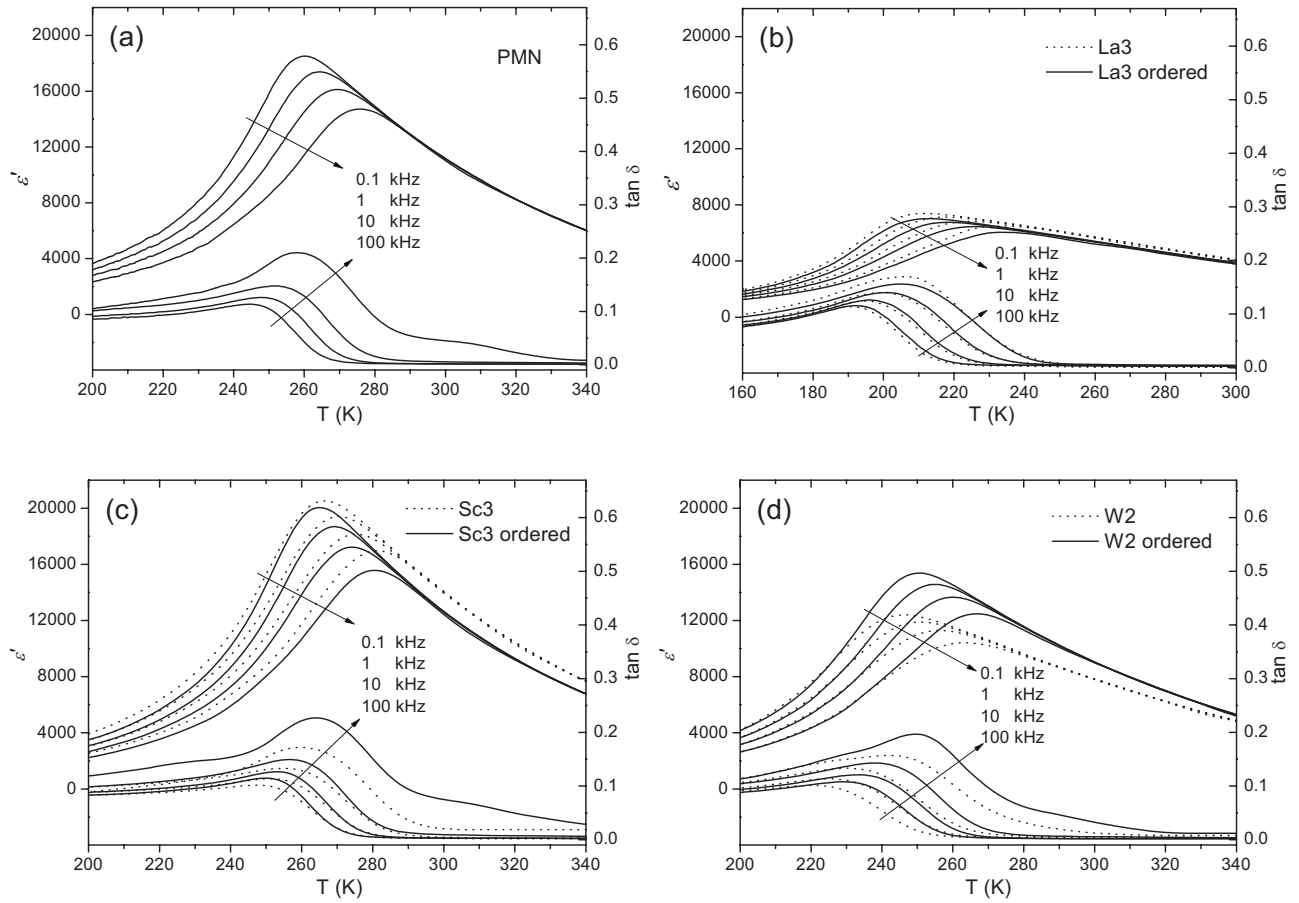

FIG. 4. Relative dielectric permittivity ε' and loss tangent tan δ as a function of temperature measured at 100 Hz, 1 kHz, 10 kHz, and 100 kHz in ceramic samples. (a) PMN, (b) La3 and La3 ordered, (c) Sc3 and Sc3 ordered, (d) W2 and W2 ordered.

The relative dielectric permittivity measured at 1 kHz is replotted in Fig. 5 for clarity. It is clear that the relative permittivity was severely suppressed and the temperature at dielectric maxima (T_m) shifted considerably to a lower temperature in both La3 and La3-ordered ceramics compared with the PMN ceramic. Almost no difference was detected in dielectric properties between La3 and La3-ordered ceramics. In the W^{6+}-doped samples, enhanced *B*-site cation order leads to a significant increase in maximum relative permittivity ε'_m and a slight shift of T_m to a higher temperature. Only slight changes both in relative dielectric permittivity and T_m were observed when comparing the Sc3 with the Sc3-ordered ceramic. The dielectric properties of all the ceramics are listed in Table II for complete comparison.

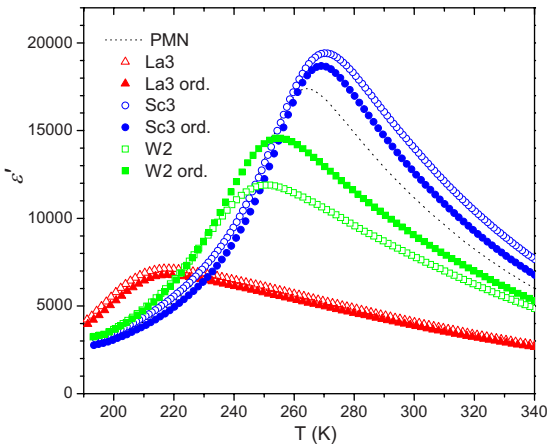

FIG. 5. (Color online) Relative dielectric permittivity ε' vs temperature at 1 kHz in all ceramic samples.

The diffuse phase transition in these relaxor ferroelectric oxides is further quantitatively characterized by evaluating the diffuseness parameter δ according to the following equation in the temperature range above T_m,[30]

$$\frac{\varepsilon_A}{\varepsilon'} = 1 + \frac{(T - T_A)^2}{2\delta^2}, \tag{1}$$

where $T_A(<T_m)$ and $\varepsilon_A(>\varepsilon'_m)$ are fitting parameters. By fitting the experimental data measured at 1 kHz with this expression, the diffuseness parameter δ can be determined. The results are also listed in Table II. With reference to the PMN ceramic, La^{3+} doping significantly increases, while Sc^{3+} doping preserves the diffuseness parameter δ. It appears that *B*-site cation order in La^{3+}-and Sc^{3+}-doped PMN ceramics does not influence the diffuseness parameter. W^{6+} doping induces a moderate increase in δ. However, the increase can be suppressed to some extent by forming large cation-ordered domains.

TABLE II. The ferroelectric properties of pure and La^{3+}, Sc^{3+}, and W^{6+}-doped PMN ceramics.

Composition	ε'_m at 1 kHz	T_m at 1 kHz (K)	δ (K)	T_{C0} (K)	Current HW2/3M (K)	T_m-T_{C0} (K)
PMN Crystal[a]	20000	265	41	215		50
PMN	17400	264	45	201	0.8	63
La3	7200	217	77	143	13	74
La3 ordered	6800	218	78	145	10	73
Sc3	19500	270	46	213	1.3	58
Sc3 ordered	18800	269	45	212	0.6	57
W2	12000	251	60	172	14	79
W2 ordered	14700	255	53	174	8	81

[a]From Refs. 4 and 12.

C. Depolarization and polarization switching

PMN-based relaxor ferroelectrics can be stabilized in several ferroelectric states under different temperature/electric field conditions.[5–12] One of the most important parameters that delineates these states is the thermal depolarization temperature T_{C0} under the "zero-field heating after field-cooling" condition, which marks a real phase transition from the induced ferroelectric phase to the ergodic relaxor phase. T_{C0} can be considered as an intrinsic property of relaxor ferroelectric materials since it is independent of the applied field strength during the "field-cooling." In the current study, T_{C0} was measured by monitoring the thermal depolarization current after the sample was cooled down to low temperatures with a dc field of 10 kV/cm. As shown in Fig. 6, very weak and broad depolarization current peaks were recorded for La^{3+}- and W^{6+}-doped ceramics. In contrast, strong and sharp peaks were detected in Sc^{3+}-doped ceramics. T_{C0} was read from Fig. 6 as the temperature at the current peaks and is also listed in Table II. To characterize the diffuseness of the ferroelectric-to-relaxor phase transition, the half width of the depolarization current peak at 2/3 maximum (HW2/3M) is determined (this choice of "diffuseness" parameter is related to the fact that the parameter δ which determines the diffuseness of the dielectric peak also represents the half-width of the peak at 2/3 maximum[2]). As indicated by the result listed in Table II, the diffuseness for the depolarization current peak increases significantly for La^{3+} and W^{6+} doping while it remains more or less the same for Sc^{3+} doping.

The difference between T_m and T_{C0} of a ferroelectric material is suggested to be indicative of the degree of long-range polar order.[27] In classical relaxor ferroelectric materials, T_{C0} is much lower than T_m, while for normal ferroelectric materials, these two temperatures converge into a single temperature, i.e., the Curie point. The measured difference of T_m and T_{C0} in all the ceramics is listed in the last column of Table II. It is evident that Sc^{3+} doping reduces the gap between the two temperatures, while La^{3+} and W^{6+} doping widen the temperature gap. In other words, compared with pure PMN, Sc^{3+} doping slightly enhances the polar order while La^{3+} and W^{6+} doping suppress the polar order. However, in ceramics with the same composition, enhanced cation order seems to have no obvious impact on this temperature gap.

The electric-field-induced polarization and polarization switching were characterized by the hysteresis loop measurement at low temperatures. The measurements recorded well-defined hysteresis loops at temperatures around and below T_{C0} for all the compositions. The results of ordered samples are shown in Fig. 7. The square hysteresis loops and the large P_r values confirm the formation of a normal ferroelectric phase under electric fields below the temperature T_{C0} in both disordered and ordered ceramics. The remnant polarization P_r and the coercive field E_c are read from the hysteresis loops and are plotted as a function of temperature in Fig. 8. As shown in Fig. 8(a), the cation-ordered samples have practically the same P_r as their disordered counterparts in the low temperature range. However, the drop of P_r with increasing temperature is comparatively sharper in the ordered samples. The coercive field E_c has been considered as the critical field for the relaxor-to-ferroelectric phase transition.[12] Figure 8(b) indicates that for all the ceramics the critical field needed for the phase transition increases dramatically with decreasing temperature.

D. Dielectric relaxation process

The relative dielectric permittivity was further measured in a wider frequency range from 10^{-2} to 10^5 Hz at selected temperatures with an impedance analyzer (Novocontrol system), as shown in Fig. 9. To reveal different relaxation processes contributing to the dielectric dispersion, the spectra were fit to analytical expressions. In all studied ceramics in the temperature range around T_m, the two main contributions to the relaxation are found similar to the PMN crystals[31] with susceptibilities χ^*_U and χ^*_{KWW}, respectively. The losses corresponding to these contributions are well resolved in frequency at comparatively high temperatures but overlap at low temperatures. In addition, two comparatively weak relaxation contributions are observed. The first of them (not found in PMN crystals[31]) can be seen in Fig. 9 in most (especially disordered) samples in the low-frequency range (0.01–10 Hz) at comparatively high temperatures. The second one appears in the measurement frequency window at comparatively low temperatures (similar to PMN crystals[31]).

The dielectric spectra can be described by the following expression:

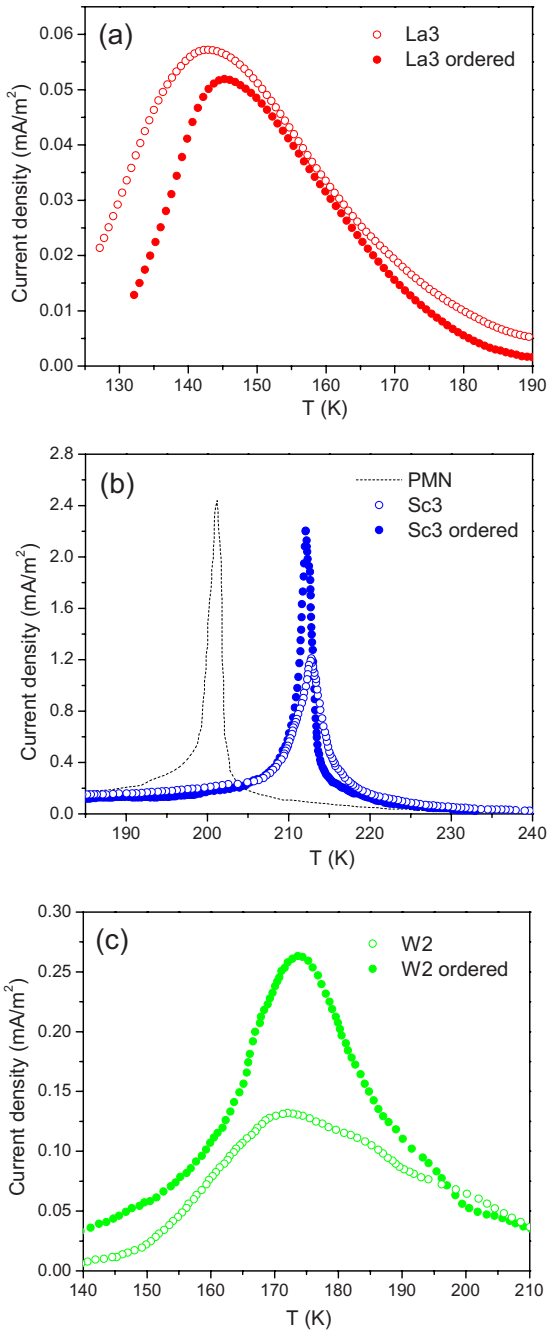

FIG. 6. (Color online) Thermal depolarization current during zero-field heating of ceramic samples after field-cooled at 10 kV/cm. (a) La3 and La3 ordered, (b) PMN, Sc3 and Sc3 ordered, (c) W2 and W2 ordered.

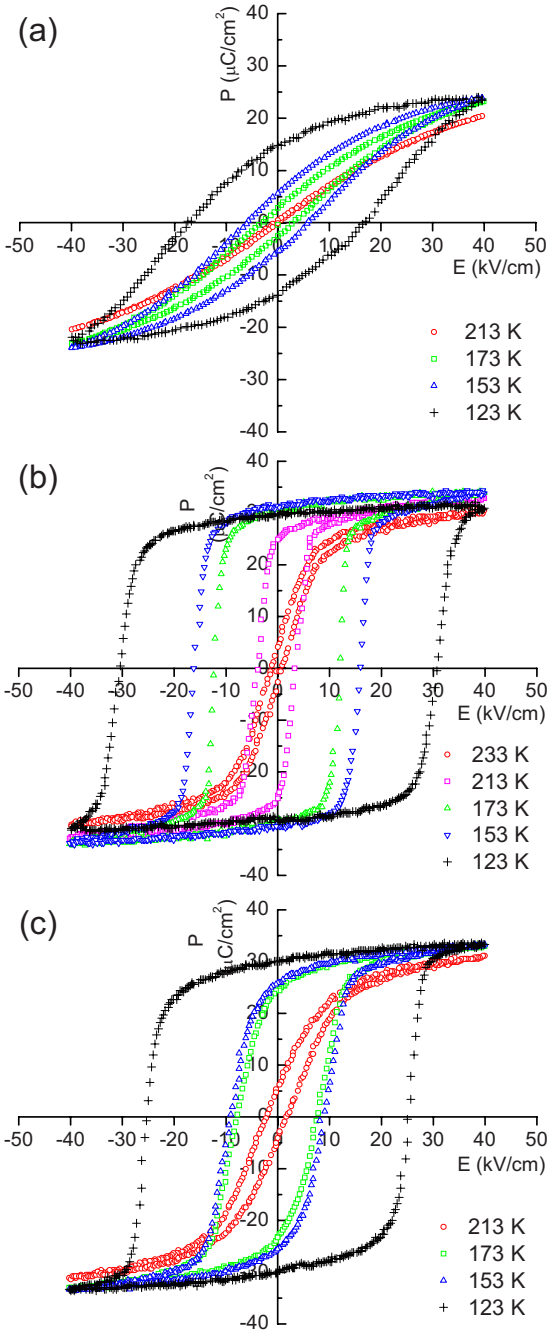

FIG. 7. (Color online) Polarization vs electric field hysteresis loops measured at 4 Hz at different temperatures. (a) La3 ordered, (b) Sc3 ordered, and (c) W2 ordered.

$$\varepsilon^*(f) = \varepsilon' - i\varepsilon'' = \varepsilon(\infty) + \chi_U^*(f) + \chi_{\mathrm{KWW}}^*(f) + \chi_{\mathrm{HN}}^*(f), \quad (2)$$

where ε^* is the measured complex relative dielectric permittivity and $\varepsilon(\infty)$ originates from other possible polarization processes exhibiting dispersion above the upper limit of the measurement frequency window. The last term, χ_{HN}^*, takes into account the aforementioned weak relaxation contributions. In accordance with Refs. 31 and 32 we express the contribution whose loss dominates at low frequencies as

$$\chi_U' = Af^{n-1}, \quad (3a)$$

$$\chi_U' = \chi_U'' \tan\left(\frac{n\pi}{2}\right), \quad (3b)$$

where A and n are the parameters. This type of susceptibility vs frequency relation was called "universal."[33] It gives a straight line with the slope determined by n when plotted in the log-log scale and represents in the frequency domain the Curie–von Schweidler (CS) relaxation law, $P \propto t^{1-n}$ (P is the

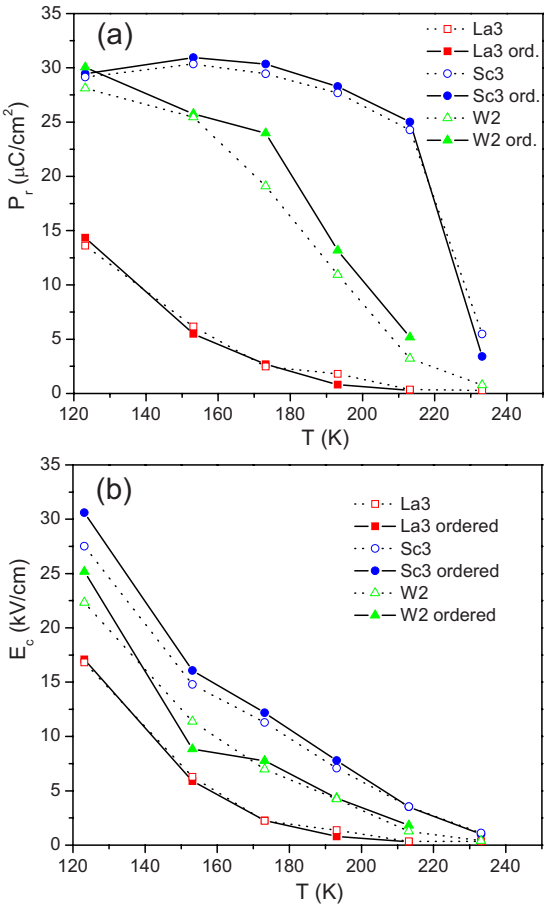

FIG. 8. (Color online) Ferroelectric properties of ceramic samples measured from the $P \sim E$ hysteresis loops. (a) Remanent polarization P_r, and (b) coercive field E_c.

polarization). The high-frequency "conventional relaxor" dispersion appears at comparatively high f. It follows the Kohlrausch-Williams-Watts (KWW) relaxation pattern, the shape of which in the time domain is described by the stretched exponential function $P(t) \propto \exp(-t/\tau_{\mathrm{KWW}})^{\beta}$ with two parameters: the characteristic relaxation time τ_{KWW} and the stretching exponent β (this symbol has nothing to do with the β' and β'' sublattices mentioned previously).

To describe two additional weak relaxations, only one term in Eq. (2) is used, which is expressed as the Havriliak-Negami (HN) relationship[33]

$$\chi^{*}_{\mathrm{HN}}(f) = \chi_{\mathrm{HN0}}[1 + (i2\pi f\tau)^{\alpha}]^{-\gamma}, \tag{4}$$

where $0 < \alpha < 1$, and $0 < \alpha\gamma < 1$ are the parameters and χ_{HN0} is the static susceptibility. It appears to be valid because each of these two contributions is important only at comparatively low and high temperatures, respectively.

Following a similar procedure described in Refs. 31 and 34, the frequency dependences of measured relative permittivity (real and imaginary parts simultaneously) are fitted at a number of fixed temperatures to Eq. (2) with the terms expressed by Eqs. (3) and (4). The frequency dependences of KWW susceptibility $\chi^{*}_{\mathrm{KWW}}(f)$ are represented by an approximate formula[31,34] with the parameters τ_{KWW} and β. The nonlinear least-squares fitting procedure was used. The best-fit relative permittivity curves are shown in Fig. 9. From this fitting the relaxation parameters are derived. For the KWW (i.e., the main) relaxation process temperature dependences of these parameters are shown in Fig. 10.

Freezing of the dielectric spectrum is characteristic of relaxor ferroelectrics. In PMN crystals freezing of KWW relaxation contribution can be described in terms of Vogel-Fulcher-type relationships[31]

$$\tau_{\mathrm{KWW}} = \tau_0 \exp\left[\frac{E_\tau}{(T - T_f)}\right], \tag{5}$$

$$\beta = \beta_0 \exp\left[-\frac{E_\beta}{(T - T_\beta)}\right], \tag{6}$$

where the parameter $T_f = T_\beta$ can be considered as the freezing temperature, i.e., the temperature where the characteristic relaxation time τ_{KWW} becomes infinite and the relaxation spectrum becomes infinitely wide ($\beta = 0$). In all ceramics studied in this work the temperature dependences of τ_{KWW} and β can be well fitted to these relationships as shown in Fig. 10. The best-fit VF parameters are listed in Table III. The VF parameters for PMN single crystals from Ref. 31 are also listed in Table III for comparison.

IV. DISCUSSION

A. Cation ordering mechanism

As evidenced by x-ray diffraction as well as TEM dark field imaging shown in Figs. 2 and 3, long-range B-site cation order was successfully developed in PMN ceramics with a dopant concentration as low as 2 or 3 at. %. However, in all the fast cooled ceramics no obvious B-cation ordering enhancement was detected. This indicates that chemical modification alone is not capable of producing significant long-range cation order. In other words, the enhanced B-site cation order observed in slow cooled samples resulted from combined chemical modification and the slow cooling procedure.

Equilibrium degree of cation order is known to be dependent on temperature.[17] In the ground state the maximum order is expected because disordering of the cations with different charges and sizes leads to increasing the internal energy (U). However, disordering leads also to increasing configurational entropy (S). As a result, at elevated temperatures (where equilibrium is determined by the minimum of free energy, U-ST) the disordered state may become equilibrium. In pure PMN the ordering temperature, T_{dis} (i.e., the temperature above which the equilibrium long-range cation order parameter equals zero), is estimated to be ~950 °C.[24] Therefore, immediately after sintering (at ~1200 °C) the ceramics should be disordered. Upon cooling below T_{dis} the ordered state becomes equilibrium. However, this state cannot be reached in practice for kinetic reasons. This is because the ordering proceeds by ionic rearrangement (diffusion) and the relaxation time of this process increases rapidly on cooling. At $T < T_{\mathrm{dis}}$ it becomes so large that no significant ordering can be achieved even after a realistically long annealing.

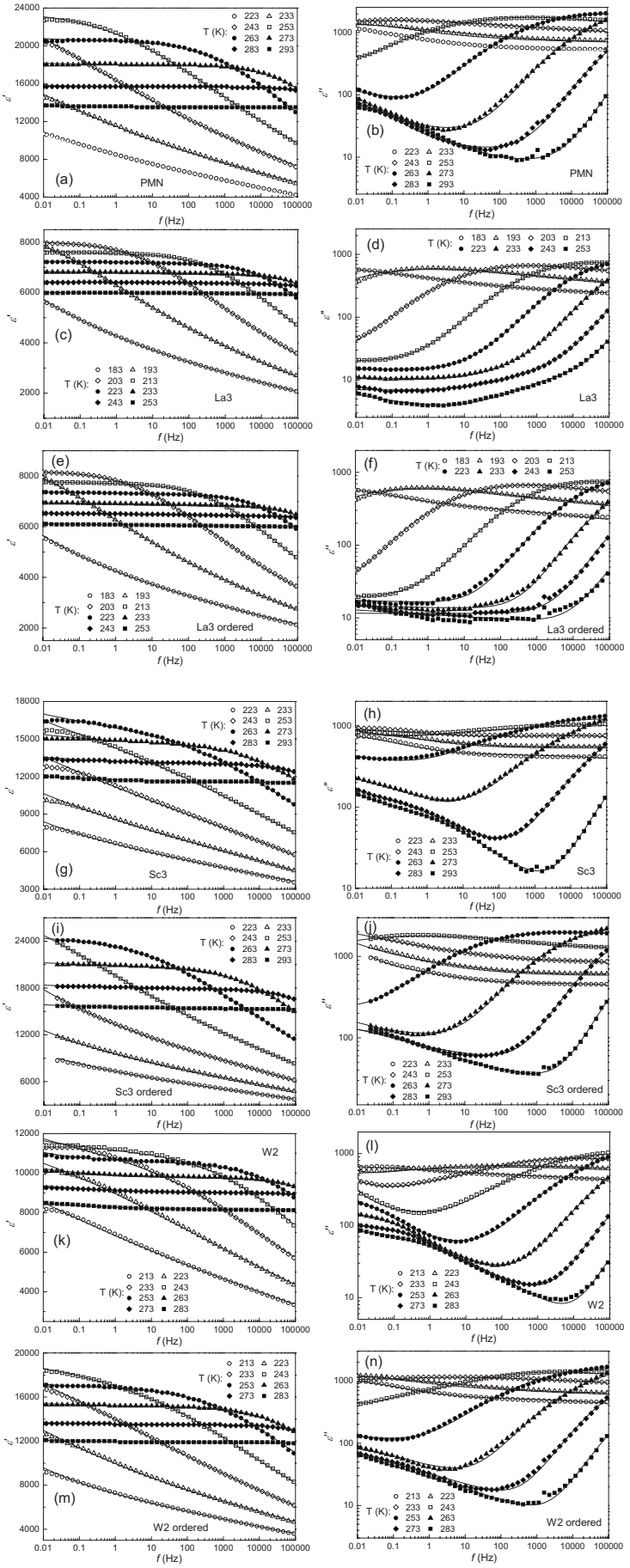

FIG. 9. Frequency dependences of the real (ε') and imaginary part (ε'') of relative dielectric permittivity at selected temperatures. Solid lines represent fitting to Eq. (2). [(a) and (b)] PMN, [(c) and (d)] La3, [(e) and (f)] La3 ordered, [(g) and (h)] Sc3, [(i) and (j)] Sc3 ordered, [(k) and (l)] W2, and [(m) and (n)] W2 ordered.

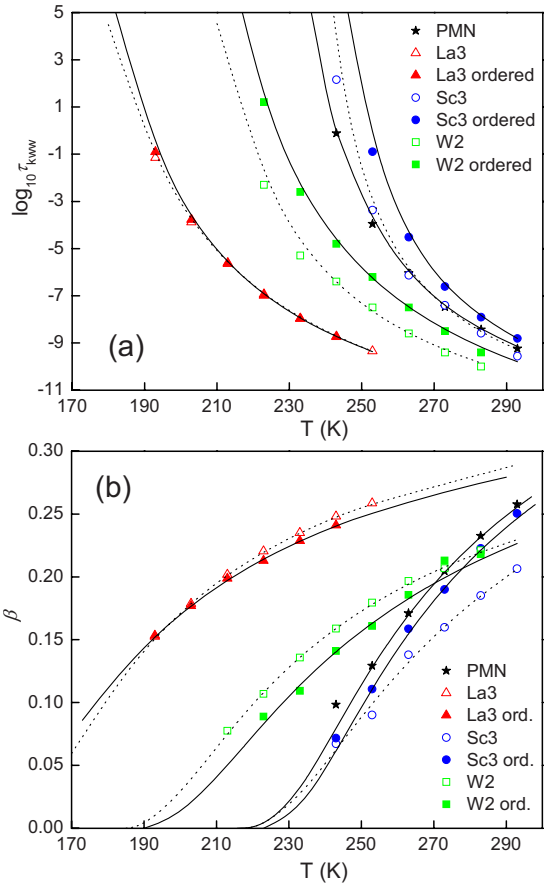

FIG. 10. (Color online) Temperature dependences of the KWW relaxation parameters in all ceramic samples. (a) The characteristic relaxation time τ_{KWW} and (b) the stretching exponent β. The fits to the VF relationships [Eqs. (5) and (6)] are shown by dashed and solid lines for disordered and ordered ceramics, respectively.

It seems that doping in our experiments increases T_{dis} and shifts it to the temperature region where the ordering relaxation time is comparatively small (in case of Sc^{3+} doping of PMN the increase in T_{dis} is confirmed experimentally[24]). Consequently, during cooling after sintering, the ordering process really proceeds in the restricted temperature interval starting from T_{dis} and below. If the sample spends comparatively long time in this interval (i.e., the cooling is slow) it attains a considerable degree of order. In case of fast cooling, the sample quickly sweeps through the temperature interval where ordering is active and thereby remains practically disordered.

The increase in T_{dis} in doped ceramics is due to the changes in the internal energy term as well as in the entropy term in free energy. The former is believed to depend on the charge and size difference of ordered cations.[35–38] In the La^{3+}-doped ceramics, La^{3+} substitutes Pb^{2+} at the A site. The smaller size of the La^{3+} cation (1.36 Å vs 1.49 Å of Pb^{2+})[39] makes the unit cell more compact. In addition, introducing La^{3+} increases the molar fraction of the larger Mg^{2+} cation on the β' sublattice. Consequently, the size difference between the β' and β'' sublattices increases and the size and charge mismatches on the β' sublattice (the random site sublattice with Mg^{2+} and Nb^{5+}) are reduced. These factors are suggested to be the primary causes for the change in the internal energy term.

In the Sc3-ordered ceramic, Sc^{3+} substitutes both Mg^{2+} and Nb^{5+} on the β' sublattice, and the β'' sublattice remains solely occupied by Nb^{5+}. The introduction of larger Sc^{3+} cations (0.745 Å vs 0.72 Å of Mg^{2+} and 0.64 Å of Nb^{5+}) increases the size difference between the β' and the β'' sublattices. In the W2-ordered sample, W^{6+} substitutes the Nb^{5+} on the β'' sublattice and increases both the charge difference and the size difference (0.60 Å of W^{6+} vs 0.64 Å of Nb^{5+}) between the two B-site sublattices. These factors are believed to facilitate the formation of large cation-ordered domains.

However, the increase in the charge and size difference between the two sublattices caused by minor doping alone can hardly account for such a significant enhancement of T_{dis} in our experiments as well as other known experimental facts.[37] Evidently, the contribution from the configurational entropy is critical and should be considered. Compositional dependence of T_{dis} in the $Pb(Mg_{1/3}Nb_{2/3})O_3$–$Pb(Sc_{1/2}Nb_{1/2})O_3$ solid solution has been calculated in the framework of the phenomenological Bragg-Williams theory which takes into account both configurational entropy and internal energy variations.[40] The calculated value of T_{dis} for Sc3 composition appears to be equal to 1070 °C, i.e., significantly larger than in pure PMN. Similar calculations applying to other solid solutions are expected to also predict a significantly increased T_{dis}.

TABLE III. The best-fit Vogel-Fulcher parameters of pure and La^{3+}, Sc^{3+}, and W^{6+}-doped PMN ceramics. Typical uncertainties are ±3, ±5, ±100, ±0.03 and ±7 K for T_f, T_β, E_τ, β_0, and E_β, respectively.

Composition	T_f (K)	T_β (K)	τ_0 (s)	E_τ (K)	β_0	E_β (K)
PMN Crystal[a]	213	210	1.6×10^{-14}	810	0.43	42
PMN	217	216	1.3×10^{-14}	831	0.48	49
La3	148	147	4.4×10^{-16}	1445	0.39	43
La3 ordered	154	141	1.4×10^{-15}	1247	0.39	48
Sc3	224	211	2.6×10^{-14}	682	0.44	62
Sc3 ordered	228	219	1.7×10^{-14}	743	0.48	50
W2	185	180	2.0×10^{-15}	1086	0.36	52
W2 ordered	184	183	1.6×10^{-16}	1500	0.40	62

[a]From Ref. 31.

B. Ferroelectric behavior and dielectric relaxation

The La3 ceramic can be considered as a solid solution between $Pb(Mg_{1/3}Nb_{2/3})O_3$ and $La(Mg_{2/3}Nb_{1/3})O_3$. $La(Mg_{2/3}Nb_{1/3})O_3$, which holds a rhombohedral perovskite structure with complete 1:1 *B*-site cation order, is a nonferroelectric material with a low relative dielectric permittivity of about 27.[41] Sc3 is a solid solution between PMN and $Pb(Sc_{1/2}Nb_{1/2})O_3$. Long-range *B*-site cation order can be developed in the complex perovskite $Pb(Sc_{1/2}Nb_{1/2})O_3$ by extended annealing. The ordered $Pb(Sc_{1/2}Nb_{1/2})O_3$ shows normal ferroelectric behavior with a sharp first-order ferroelectric to paraelectric transition occurring at 78 °C.[16] $Pb(Mg_{1/2}W_{1/2})O_3$ is an antiferroelectric perovskite with a complete Mg:W cation order, a Curie point at 39 °C, and a relative dielectric permittivity of 150 at room temperature.[42] W2, therefore, is a solid solution between a relaxor and an antiferroelectric.

As shown in Figs. 5 and 6, extended thermal treatment at elevated temperatures and change in chemical composition lead to noticeable changes in properties. It should be pointed out that all the doped ceramics (disordered and ordered) have comparable grain sizes. Therefore, it is reasonable to assume that the observed changes in the behavior originate from the development of cation order. Furthermore, the relaxation parameters in the PMN ceramic are found to be practically the same as in PMN crystals (Table III). This fact indicates that the crystalline grain interior is responsible for the relaxation process; the contribution of grain boundaries is negligible and the difference of relaxation parameters should be attributed to the variation in composition or the degree of cation disorder rather than to other variables such as grain size and density.

Qualitatively the dielectric behavior in all studied ceramics is the same as in prototypic relaxor ferroelectric PMN, namely, the high-temperature slope of the $\varepsilon'(T)$ peak follows the quadratic law [Eq. (1)] while the main contribution to the peak comes from the KWW relaxation process ("conventional relaxor" dielectric response). The temperature dependences of the dielectric relaxation time τ_{KWW} and KWW parameter β (which characterizes the broadness of relaxation spectrum) are described by VF-type relations [Eqs. (5) and (6)]. The VF temperatures T_f and T_β are close to each other, which implies a glassy freezing at T_f (τ_{KWW} becomes infinitely large and the spectrum becomes infinitely wide at this temperature).[31] The mechanism of this relaxation is commonly attributed to the flipping of PNRs which exist in the ergodic relaxor phase (in a wide temperature range around T_m).[2–4,31]

Cation ordering does not change the dielectric response significantly. Indeed, as one can see in Fig. 10, at a fixed temperature the relaxation parameters τ_{KWW} and β are the same or very close in ordered and disordered samples of the same composition. Accordingly, the VF parameters T_f, τ_0, E_τ, T_β, E_β, and β_0 are practically the same in the disordered samples as in their partially ordered counterparts (see Table III). The parameters of the quadratic relationship [Eq. (1)] which describes the temperature dependence of the static relative dielectric permittivity are also very close (moderate changes are observed only in the W2 composition).

The independence of dielectric response from the degree of cation order, which we observed here in doped PMN-based relaxors, presents a striking contrast to the behavior of $Pb(B'_{1/2}B''_{1/2})O_3$-type relaxors where cation ordering causes significant variation in the temperature and diffuseness of the dielectric peak as well as the dielectric dispersion.[3,9,13,16–22] Our results are unexpected in the framework of some previous approaches and theories. In particular, it was suggested[13] that the cation-ordered regions with the size of several nanometers act as sites to localize the dynamic PNRs and therefore the relaxor behavior should be observed only in those compounds where the cation-ordered nanoregions were present. The similar conclusion has been recently derived theoretically using first-principles-based simulations.[14] In our partially ordered samples the cation-ordered regions are rather large (~100 nm), but relaxor-type dispersion persists, and furthermore, the relaxation parameters are practically the same as in pure PMN where cation-ordered regions are of the nanometer size.

In contrast to small-signal dielectric properties, cation ordering significantly modifies the diffuseness of the ferroelectric phase transition at T_{C0}: the depolarization current HW2/3M value in the disordered Sc3 ceramic is more than twice as large as in the partially ordered one. The same trend is observed in other compositions (see Table II). A more abrupt decrease in the remanent polarization around T_{C0} with increasing temperature in the ordered samples can be seen in Fig. 8(a).

Note that relaxor ferroelectrics are also called, especially in early literature,[1,2] the "ferroelectrics with diffuse phase transitions," and the diffuseness of the $\varepsilon'(T)$ peak is often used as an estimate for the diffuseness of the ferroelectric phase transition. Our results suggest that the formation of PNRs and the transition to the ferroelectric phase are relatively independent events. This behavior can be understood in the framework of the phenomenological two-stage kinetic model of diffuse phase transitions in disordered crystals.[12,43] The model suggests the existence of two temperature intervals for the evolution of polar structure in relaxors. PNRs are formed in the course of cooling in the first stage (within the temperature interval of the ergodic relaxor phase). In the second stage (at lower temperatures) the growth of PNRs into comparatively large ferroelectric domains (i.e., ferroelectric phase transition) may begin, which can be either a sharp or a diffuse process. In different stages the process is governed by different factors. The formation of PNRs is determined by the quenched short-range cation disorder (as described in some microscopic models, see Ref. 44), while mesoscopic quenched inhomogeneities and interactions between PNRs play a significant role in the development of low-temperature ferroelectric or nonergodic relaxor phases. Equality of the relaxation parameters and the dielectric peak diffuseness δ in our samples with different sizes of cation-ordered regions implies equality of the PNR system (which is known to be responsible for dielectric relaxation in the ergodic relaxor phase). On the other hand, the difference in the behavior around T_{C0} implies some differences on the mesoscopic scale.

To account for our observations we apply the approach used previously to describe the properties of La^{3+}-doped PMN crystals.[45] It was assumed that the dynamic PNRs are located in the cation disordered matrix, while polar regions which appear in the places of cation-ordered regions are static and cannot contribute to the small-signal dielectric response. The structure of the disordered matrix does not vary significantly during cation ordering; therefore, the properties of dynamic PNRs and the dielectric relaxation parameters remain almost unchanged. On the other hand, the size of cation-ordered regions vary dramatically (from several nanometers in the disordered samples to ~100 nm in the partially ordered ones). The size and thereby the properties of static polar regions are expected to vary accordingly. Large electric fields applied in the field-cooling experiments are able to reorient static polar regions (or at least some of them). Therefore, the remanent polarization (and the depolarization current in the course of zero-field heating after field cooling) is determined not only by the dynamic PNRs frozen at low temperatures but also by the static polar regions. The smaller diffuseness of the ferroelectric phase transition in ordered ceramics is related to the ordering-induced changes (in particular, the size increase) of the static polar regions.

V. CONCLUSIONS

Large (~100 nm) domains of long-range *B*-site cation order are observed by TEM in $Pb(Mg_{1/3}Nb_{2/3})O_3$ ceramics doped with only 2 or 3 at. % of La^{3+}, Sc^{3+}, or W^{6+} and slowly cooled (10 °C/hour) after sintering at 1200 °C–1250 °C. The development of long-range cation ordering (which is known to be impossible in pure PMN) is attributed to the increase in the temperature of the cation order-disorder transition caused by chemical doping. Comparison of the properties between ordered and disordered ceramics of the same compositions shows that cation ordering does not influence significantly the small-signal dielectric response. In particular, glassy freezing of the dielectric spectrum is revealed practically at the same temperature and the diffuseness of the characteristic relaxor $\varepsilon'(T)$ peak is essentially the same in the ordered and disordered samples. The effect of cation ordering on the temperature T_{C0} of the phase transition from the ferroelectric phase (induced by a large external electric field) to the ergodic relaxor phase is also small (within 1–2 K). However, the diffuseness of this phase transition appears to be much larger in the disordered samples than in the ordered ones, as determined from the pyroelectric current and the ferroelectric hysteresis loops measurements. This behavior can be related to the existence of different types of polar regions in doped PMN ceramics. Polar nanoregions giving rise to the small-signal dielectric response are located in the disordered matrix (outside cation-ordered domains), which is the same in the ordered and disordered samples. Polar regions (ferroelectric domains) located in the cation-ordered domains are static and, therefore, cannot contribute to the small-signal response. However, their contribution to the remanent polarization (which determines in particular the pyroelectric current) is significant and changes with the size of the cation-ordered domains.

ACKNOWLEDGMENTS

This work was supported by the National Science Foundation through the CAREER Grant No. DMR-0346819 (X.T.) and by the Office of Naval Research through Grant No. 00014-06-1-0166 (Z.G.Y.).

*Authors to whom correspondence should be addressed; xtan@iastate.edu ; zye@sfu.ca

[1] G. A. Smolenskii and A. I. Agranovskaya, Sov. Phys. Tech. Phys. **3**, 1380 (1958).
[2] G. A. Smolenskii, J. Phys. Soc. Jpn. **28** (Suppl.), 26 (1970).
[3] L. E. Cross, Ferroelectrics **76**, 241 (1987).
[4] A. A. Bokov and Z.-G. Ye, J. Mater. Sci. **41**, 31 (2006).
[5] R. Sommer, N. K. Yushin, and J. J. van der Klink, Phys. Rev. B **48**, 13230 (1993).
[6] Z. G. Ye and H. Schmid, Ferroelectrics **145**, 83 (1993).
[7] E. V. Colla, E. Y. Koroleva, N. M. Okuneva, and S. B. Vakhrushev, Phys. Rev. Lett. **74**, 1681 (1995).
[8] Z. G. Ye, Ferroelectrics **184**, 193 (1996).
[9] Z. G. Ye, Key Eng. Mater. **155-156**, 81 (1998).
[10] B. Dkhil and J. M. Kiat, J. Appl. Phys. **90**, 4676 (2001).
[11] B. E. Vugmeister and H. Rabitz, Phys. Rev. B **65**, 024111 (2001).
[12] X. Zhao, W. Qu, X. Tan, A. A. Bokov, and Z.-G. Ye, Phys. Rev. B **75**, 104106 (2007).
[13] C. A. Randall and A. S. Bhalla, Jpn. J. Appl. Phys., Part 1 **29**, 327 (1990).
[14] B. P. Burton, E. Cockayne, and U. V. Waghmare, Phys. Rev. B **72**, 064113 (2005).
[15] M. A. Akbas and P. K. Davies, J. Am. Ceram. Soc. **80**, 2933 (1997).
[16] C. G. F. Stenger and A. J. Burggraaf, Phys. Status Solidi A **61**, 653 (1980)
[17] A. A. Bokov, Ferroelectrics **183**, 65 (1996).
[18] A. A. Bokov, I. P. Rayevskii, and V. G. Smotrakov, Fiz. Tverd. Tela (Leningrad) **25**, 2025 (1983) [Sov. Phys. Solid. State **25**, 1168 (1983)].
[19] A. A. Bokov, M. A. Leshchenko, M. A. Malitskaya, and I. P. Raevski, J. Phys.: Condens. Matter **11**, 4899 (1999).
[20] F. Chu, N. Setter, and. A. K. Tagantsev, J. Appl. Phys. **74**, 5129 (1993).
[21] D. Viehland and J.-F. Li, J. Appl. Phys. **75**, 1705 (1994).
[22] A. A. Bokov, V. Y. Shonov, I. P. Rayevsky, E. S. Gagarina, and M. F. Kupriyanov, J. Phys. Condens. Matter. **5**, 5491 (1993).
[23] J. Chen, H. M. Chan, and M. P. Harmer, J. Am. Ceram. Soc. **72**, 593 (1989).
[24] L. Farber, M. Valant, M. A. Akbas, and P. K. Davies, J. Am. Ceram. Soc. **85**, 2319 (2002).
[25] L. Farber and P. K. Davies, J. Am. Ceram. Soc. **86**, 1861 (2003).
[26] L. J. Lin and T. B. Wu, J. Am. Ceram. Soc. **73**, 1253 (1990).

[27] X. H. Zhao, W. G. Qu, H. He, N. Vittayakorn, and X. Tan, J. Am. Ceram. Soc. **89**, 202 (2006).
[28] S. Nomura, S. J. Jang, L. E. Cross, and R. E. Newnham, J. Am. Ceram. Soc. **62**, 485 (1979).
[29] S. L. Swartz and T. R. Shrout, Mater. Res. Bull. **17**, 1245 (1982).
[30] A. A. Bokov and Z.-G. Ye, Solid State Commun. **116**, 105 (2000).
[31] A. A. Bokov and Z.-G. Ye, Phys. Rev. B **74**, 132102 (2006).
[32] A. A. Bokov and Z.-G. Ye, Phys. Rev. B **65**, 144112 (2002).
[33] A. K. Jonscher, *Universal Relaxation Law* (Chelsea Dielectric, London, 1996).
[34] A. A. Bokov, A. Hilczer, M. Szafrański, and Z.-G. Ye, Phys. Rev. B **76**, 184116 (2007).
[35] F. Galasso and M. Darby, J. Phys. Chem. **66**, 131 (1962).
[36] A. A. Bokov, N. P. Protsenko, and Z. G. Ye, J. Phys. Chem. Solids **61**, 1519 (2000).
[37] P. K. Davies and M. A. Akbas, J. Phys. Chem. Solids **61**, 159 (2000).
[38] X. Zhao, W. Qu, and X. Tan, J. Am. Ceram. Soc. **91**, 3031 (2008).
[39] R. D. Shannon, Acta Crystallogr. Sect. A: Cryst. Phys., Diffr., Theor. Gen. Crystallogr. **32**, 751 (1976).
[40] I. P. Raevski, S. A. Porsandeev, S. M. Emelyanov, V. G. Smotrakov, V. V. Eremkin, I. N. Zakharchenko, S. I. Raevskaya, E. S. Gagarina, F. I. Savenko, and E. V. Sahkar, Ferroelectrics **298**, 267 (2004).
[41] J. H. Paik, C. H. Choi, S. Nahm, J. D. Byun, and H. J. Lee, J. Mater. Sci. Lett. **18**, 889 (1999).
[42] C. H. Lu, J. Mater. Sci. **31**, 699 (1996).
[43] A. A. Bokov, Ferroelectrics **190**, 197 (1997).
[44] T. Egami, Ferroelectrics **267**, 101 (2002).
[45] X. Long, A. A. Bokov, Z.-G. Ye, W. Qu, and X. Tan, J. Phys.: Condens. Matter **20**, 015210 (2008).